Journal of Asian Earth Sciences 73 (2013) 252–262

Contents lists available at SciVerse ScienceDirect

Journal of Asian Earth Sciences

journal homepage: www.elsevier.com/locate/jseaes

Electromagnetic emissions during dilating fracture of a rock

Tao Zhu [a,b,*], Jianguo Zhou [a], Hongqiang Wang [a]

[a] Key Laboratory of Seismic Observation and Geophysical Imaging, Institute of Geophysics, China Earthquake Administration, Beijing 100081, China
[b] State Key Laboratory of Earthquake Dynamics, Institute of Geology, China Earthquake Administration, Beijing 100029, China

ARTICLE INFO

Article history:
Received 15 August 2012
Received in revised form 18 April 2013
Accepted 3 May 2013
Available online 15 May 2013

Keywords:
Electromagnetic emission
Electromagnetic signal
Dilating fracture
Electromagnetic experiment

ABSTRACT

A lot of experiments on electromagnetic emissions (EMEs) have been reported under axial compressive fracture, shear fracture, indentation fracture and stick–slip (friction) in lab and blasting in situ, but there are rare reports on the in-lab experimental work on EMEs during dilating fracture of a rock which is helpful in studying and understanding EMEs related to slow earthquakes and the earthquakes due to volcanic activities and water level changes of reservoirs. Therefore, in the present paper in order to check whether there are detectable EMEs during dilating fracture of a rock in lab, dilating fracture experiments were conducted. The dry cuboid specimens of initially intact granodiorite and limestone were tested inside magnetic field free space (MFFS) at room temperature. We arranged evenly 20 EME antennas whose resonance frequencies range from 2.5 kHz to 540 kHz close to rock specimens. Our experimental results strongly indicate that detectable EMEs could generate during dilating fracture of a rock. They were recorded only associated with some but not all phases of fracture. Their waveforms often took on the trend that a peak arrived at first and then attenuated sharply and followed by a series of low-amplitude oscillations. The electromagnetic (EM) signals after eliminating the effects of EME antennae via deconvolution had the maximum peak-to-peak amplitudes of about 80.0 mV and 40.5 mV for granodiorite and limestone, respectively. Their main spectral components often concentrated in the band of several kHz to ~60 kHz and of several kHz to ~280 kHz. The emission of electrons and charged particles from fracture surfaces and/or micro-fracture electrification could be possible mechanisms for our experimental results.

1. Introduction

EMEs from materials fractured under stress were first observed by Stepanov in 1933, but the studies on EME in rocks did not begin until an EM anomaly was discovered prior to an earthquake by seismic researchers in 1980s (He et al., 2012). More and more EM anomalies associated with earthquakes have been observed in the lithosphere, atmosphere and ionosphere (e.g. Gokhberg et al., 1982; Tate and Daily, 1989; Fraser-Smith et al., 1990; Qian et al., 2001; Hayakawa and Molchanov, 2000; Nagao et al., 2002; Yu et al., 2010; Huang, 2011; Rong et al., 2012), and they have been also detected in coal or rock dynamic disasters occurring frequently in China coal mines in recent years (e.g. Wang et al., 2005, 2011; Jia et al., 2009), so EME has attracted much attention from the researchers all over the world. In order to comprehend EME and explore the new method for prediction of earthquakes and coal or rock dynamic disasters, a lot of experiments on hard rocks (such as granite, quartzite, limestone, basalt, and marble), soft rocks (such as coal, sandstone, and mudstone) and other materials (such as concrete, glass, and man-made samples) have been performed under different experiment conditions (e.g. Nitsan, 1977; Warwick et al., 1982; Yamada et al., 1989; Qian et al., 1996; Rabinovitch et al., 2000; Wang and He, 2000; Freund, 2002; Yoshida and Ogawa, 2004; Tsutsumi and Shirai, 2008; Jia et al., 2009; Onuma et al., 2011; Wang et al., 2011; He et al., 2012). Their main experimental results are summarized as follows: (1) EME has a very wide frequency range which covers from VLF to visible light (e.g. Nitsan, 1977; Sun et al., 1986; Qian et al., 1996; Cress et al., 1987; Yamada et al., 1989) for hard rock while from low frequency to X-ray light for soft rock, especially gas-containing coal or rock (He et al., 2012). (2) There is a positive relationship between the intensity and count of EME and load and a negative relationship between the amplitude of EME and the distance of an EME antenna to a fracture (e.g. Jia et al., 2009; He et al., 2012). (3) EMEs are in or not in sync with acoustic emissions (AEs) and are not always found with AEs (e.g. Yoshida and Ogawa, 2004; Mori et al., 2009; Sun et al., 1986). (4) EM signals recorded by the different-frequency antennas placed at different positions are not in sync (e.g. Qian et al., 1998; Stavrakas et al., 2007). Based on these experimental results, several models have been proposed to explain the universal features of the generation of EM signals from rocks,

* Corresponding author at: Key Laboratory of Seismic Observation and Geophysical Imaging, Institute of Geophysics, China Earthquake Administration, Beijing 100081, China. Tel.: +86 10 68729112.
E-mail address: zhutao197328@gmail.com (T. Zhu).

1367-9120/$ - see front matter © 2013 Elsevier Ltd. All rights reserved.
http://dx.doi.org/10.1016/j.jseaes.2013.05.004

including piezoelectric effect (Nitsan, 1977; Yoshida et al., 1997), electrokinetic effect (Mizutani et al., 1976; Ren et al., 2012), micro-fracture electrification (Ogawa et al., 1985; Molchanov and Hayakawa, 1995, 1998), the emission of electrons and charged particles from fracture surfaces (Enomoto and Hashimoto, 1990), atomic oscillations upon crack surfaces (Frid et al., 2003), the bombardment of atmospheric gases due to the turbulent flow of net charged particles (Cress et al., 1987), and compressed atom and electron emission (Guo et al., 1989). However, these results and models have been based mainly on the experiments under axial compressive fracture, shear fracture, indentation fracture and stick–slip (friction) in lab and blasting in situ. Aside from these experiments, the amount of experimental work on dilating fracture remains relatively limited.

Hao et al. (2003) recorded the self-potential and ULF magnetic field during the dilating fracture of a granodiorite, but they did not record EME, which leads to the following questions. Could detectable EME generate during dilating fracture of a rock? If it could, what frequency features does it have? In order to address them, we conducted the dilating fracture experiments on two sets of granodiorite samples and one set of limestone samples in the MFFS at room temperature and measured EMEs associated with rock fracture in the present study. We recorded the waveforms of EMEs during dilating fracture and analyzed their spectral components using FFT. This paper described the characteristics of the recorded EM signals.

2. Experimental procedure

The rock specimens used in our dilating fracture experiments were intact granodiorite and limestone from Fangshan District, Beijing, China. During the experiments, we measured strains, AEs and a series of frequency components of EMEs.

As shown in Fig.1a, a cuboid rock specimen was placed on the isolated platform inside the MFFS. The MFFS was constructed by the Institute of Geophysics, China Earthquake Administration and is a hollow near-spherical polyhedron with 26 faces consisting of 8-layer permalloy 1J85 for shielding magnetic fields and 2-layer purified aluminium for shielding electric fields. It is about 2.3 m in diameter and mainly shields static magnetic field by a factor of 160–4000 for the 0.01–10 Hz magnetic signals (Table 1) (Zhou et al., 1995) and a factor larger than 4000 for the 10 Hz to 1 kHz ones (Private communication with professor Xun Zhou who was in charge of the construction and testing of the MFFS). The intensity of the magnetic field inside the space is less than 20 nT and fluctuates less than 0.3 nT in 90 h (Zhou et al., 1995). Three holes were drilled along the longer central line on the top plane of a specimen (Fig. 1b) in order to generate facture almost along the central line. There were about 3.3 cm for the central hole and about 2.5 cm for the other two holes in diameter. The distance was about 5.5 cm from the central hole to any one of the other two holes. The depths of all three holes were about two third of the height of a rock specimen.

Three resistance strain gauges and two resonant AE sensors with the resonance frequency of 1 MHz were directly stuck on the surface of a rock specimen. 20 EME antennae with the resonance frequencies from 2.5 kHz to 540 kHz were arranged evenly with the spacing of about 2 cm. The distance of each EME antenna to the surface of a specimen was about 3 cm (Fig. 1b). 3 EME antennas (EME21, EME22 and EME23) with resonance frequencies of 6.5 kHz, 28.4 kHz and 339.0 kHz respectively were placed outside but near the MFFS for the elimination of EM disturbance signals via comparison.

EME antennas were cylindrical ferrite rods wound with 50–10,000 turns of enameled Cu wires (0.08 mm or 0.22 mm in diameter). These cylindrical ferrite rods were 120 mm, 100 mm or 70 mm in length and 10 mm in diameter and the magnetic permeability of 400 μH/m (Table 2). We calibrated the frequency responses and resonance frequencies of these EME antennas using a standard solenoidal coil with the diameter of 60 cm and the calibration factor of 152 nT/mA, a signal generator (Agilent 33250A) and an oscilloscope (Tektronix TDS1002B) and abiding by the following procedures. Firstly, an EME antenna was arranged horizontally at the center of the standard solenoidal coil placed near the

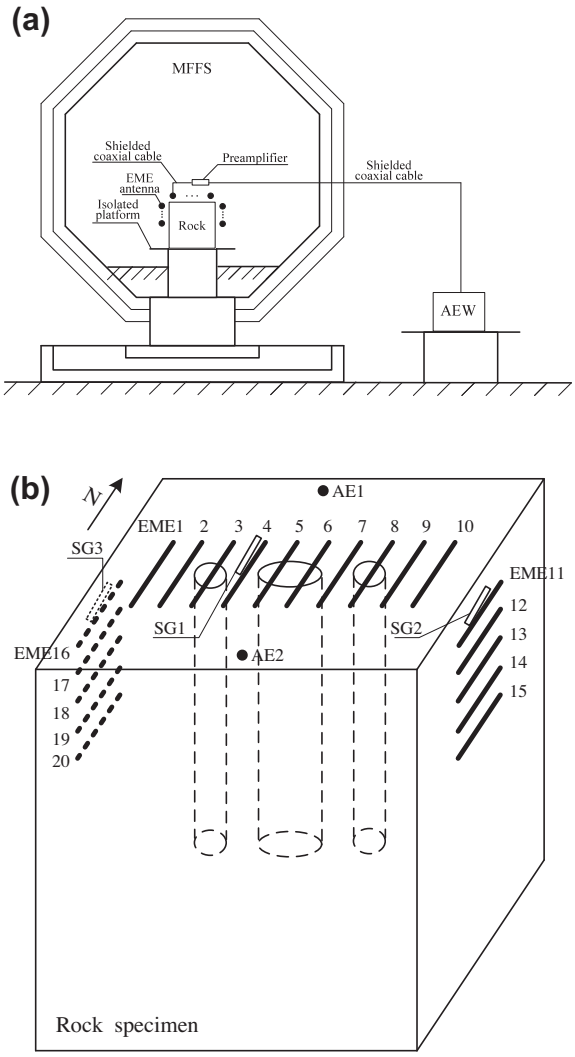

Fig. 1. The scheme of experimental configuration and the arrangement of strain gauges, AE sensors and EME antennas. AE1 and AE2 indicate resonant AE sensors. EME1-20 indicate EME antennas. SG1-3 indicate resistance strain gauges. EME1-20 have the resonance frequencies of 2.9 kHz, 4.1 kHz, 7.0 kHz, 9.4 kHz, 27.4 kHz, 101.0 kHz, 224.0 kHz, 330.0 kHz, 540.0 kHz, 433.0 kHz, 2.5 kHz, 3.5 kHz, 6.9 kHz, 10.1 kHz, 27.4 kHz, 103.0 kHz, 225.0 kHz, 334.0 kHz, 500.0 kHz and 390.0 kHz respectively.

Table 1
The shielding factors of the MFFS for different frequency magnetic signals (Zhou et al., 1995).

Frequency range	Shielding factor
0.01–0.5 Hz	160–200
0.5–1.0 Hz	200–400
1.0–2.0 Hz	400–1000
2.0–10.0 Hz	1000–4000
>10.0 Hz	>4000